Structure and microwave properties of $Fe_{75}Si_{25}$ alloys produced by high-energy wet ball milling in organic media

K. A. Yazovskikh[1,†], S. F. Lomayeva[1], A. A. Shakov[1], G. N. Konygin[1], O. M. Nemtsova[1],

A. O. Shiryaev[2], D. A. Petrov[2], K. N. Rozanov[2]

†k.yazovskikh@bk.ru

[1]Udmurt Federal Research Center UB RAS, 132 Kirov str., Izhevsk, 426000, Russia
[2]Institute for Theoretical and Applied Electromagnetics RAS, 13 Izhorskaya str., Moscow, 101000, Russia

Fe-Si alloys are known for excellent soft magnetic properties and are widely used as fillers of composites for microwave applications. A change in the size and morphology of powder particles has a significant effect on the microwave properties of composites filled with such powders. In this paper, $Fe_{75}Si_{25}$ powders were produced by high-energy wet ball milling in organic media. A solution of stearic acid in petroleum ether (a surfactant solution) and acetone were used as milling media. The effect of wet ball milling conditions on the morphology and structure of the produced powders was studied by electron microscopy, X-ray diffraction, Mössbauer spectroscopy and X-ray photoelectron spectroscopy. The use of a surfactant solution and acetone as milling media promotes the plasticization of the brittle alloy $Fe_{75}Si_{25}$ and the formation of flat particles. The wet ball milling of the alloy in acetone leads to the formation of particles of a much larger thickness and smaller size in comparison to the particles produced by wet ball milling in a surfactant solution. In both cases, after milling the alloy is disordered. During the milling process the Si concentration in the alloy decreases due to the formation of surface oxide layers enriched with silicon. The frequency dependence of microwave permittivity and permeability of composites filled with produced powders was studied. The depolarization factor, percolation threshold and intrinsic permeability of produced powder particles were determined. The frequency dependence of intrinsic permeability of the particles was shown to depend strongly on the milling conditions. A change in the milling conditions makes it possible to produce $Fe_{75}Si_{25}$ powders with the required microwave properties.

Keywords: $Fe_{75}Si_{25}$ alloy, high-energy milling, liquid organic medium, composites, effective permeability, intrinsic permeability.

1. Introduction

By now, nanocrystalline Fe-Si alloys produced by ball milling have been studied in detail in a wide range of Si concentrations. These alloys known for excellent soft magnetic properties are characterized by high values of permeability, a low coercive force, and are widely used in various applications [1 – 5]. The microwave properties of composites filled with stone-like $Fe_{75}Si_{25}$ particles were investigated in [6]. The particles were produced by the ball milling of the $Fe_{75}Si_{25}$ stoichiometric alloy in an argon atmosphere. A change in the shape and the size of the particles in the milling process has a significant influence on the high-frequency properties of composites filled with such powders [7 – 12]. It is possible to produce powder particles of the required size and shape with minimal changes in the phase composition of the material by varying the parameters of the milling process and composition of the milling medium [13]. From this point of view, the effect of wet ball milling (WBM) conditions on the change in the morphology and microwave properties of Fe-Si-based alloys is of interest. In this paper, samples were produced by WBM of the $Fe_{75}Si_{25}$ alloy in the presence of a surfactant and in an acetone medium.

The paper focuses on the structural characterization of the $Fe_{75}Si_{25}$ alloys and the microwave properties of the composites filled with the produced powders.

2. Materials and methods

Sample 1 was produced by the WBM of the stoichiometric $Fe_{75}Si_{25}$ alloy in a surfactant solution (3 wt. % stearic acid dissolved in petroleum ether) for 12 hours. Initial $Fe_{75}Si_{25}$ alloy was prepared by induction melting (sample 1*).

Sample 2 was produced from the elemental powder mixture containing 75 at. % Fe and 25 at. % Si in two successive stages: by ball milling in an argon atmosphere for 40 hours; and then by wet ball milling in acetone for 5 hours.

WBM was carried out using a Fritsch planetary ball mill. Vials and balls were made of hardened steel containing 1.5 wt. % Cr, 1 wt. % C. The weight ratio of the balls to the powder was close to 10 : 1.

Electron microscopy studies were conducted using a Hitachi Tabletop Microscope TM-1000 and a VEGA 3 LMH (TESCAN) scanning electron microscope.

The X-ray diffraction (XRD) analysis was performed with a MiniFlex Rigaku diffractometer (CoK_α-radiation). X-ray patterns were analyzed using software packages [14].

The X-ray photoelectron spectra (XPS) were measured with an ES-2401 X-ray photoelectron spectrometer.

The Mössbauer spectra were measured with a SM2201DR spectrometer in the constant acceleration mode with ^{57}Co source embedded in the Cr matrix. The hyperfine magnetic field distribution functions $P(H)$ were found using the generalized regular algorithm [15].

To conduct the microwave measurements, composites with various concentrations of the produced powders were made. Paraffin wax was used as a dielectric matrix of the composites. The measurements of the complex microwave permeability and permittivity of the composites were performed by the Nicolson-Ross-Weir technique [16] using a standard N-type coaxial airline with the torus-shaped sample filling the cross section of the airline. The measurements of the reflection and transmission coefficients of the airline with the sample were made with an HP 8720 vector network analyzer in a frequency range of 0.1 to 20 GHz. The length of the samples was about 2 mm.

All measurements were carried out at room temperature.

3. Results and discussion

3.1. Structural characterization

Fig. 1 shows electron microscopic images of the particles of samples. The typical morphology of $Fe_{75}Si_{25}$ particles mechanically alloyed in a protective argon atmosphere is represented by stone-like agglomerates [6]. WBM promotes the plasticization of the brittle $Fe_{75}Si_{25}$ alloy. Adsorption of surfactant on the newly formed alloy surface during milling prevents cold welding of particles. Thus, the typical morphology of powder particles of sample 1 is represented by plate-like particles approximately 0.5 μm in thickness (Fig. 1a).

WBM in an acetone medium contributes to the production of plate-like particles with sizes up to 10 μm (Fig. 1b). This treatment leads to a narrower particle size distribution compared to sample 1. The thickness of the particles after milling in an acetone medium is larger than the thickness of the particles after surfactant-assisted milling (approximately 2 μm). The shape of some particles is stone-like.

The results of XRD analysis of samples are shown in Fig. 2 and Table 1. (111) and (200) superstructure reflexes are observed in the X-ray pattern of the initial sample 1*, which indicates $D0_3$-type ordering (Fig. 2a). Broadened bcc reflections are observed in the X-ray pattern of samples (Fig. 2b, c). $D0_3$-type superstructure reflections are absent, which indicates that the alloys are disordered.

Table 1 shows the lattice parameters of the samples and the Si concentration in the samples according to the concentration dependences of the lattice parameter of ordered and disordered Fe-Si alloys [17, 18]. In accordance with [18], the lattice parameter of sample 1 corresponds to 22 at.% silicon concentration in the alloy, which is lower than the initial silicon concentration, 25 at.%. The silicon concentration in alloy 2 (15 at.%) is also lower than the initial one.

The quantitative analysis of the XPS spectra shows that the surface layer of the samples is enriched in silicon
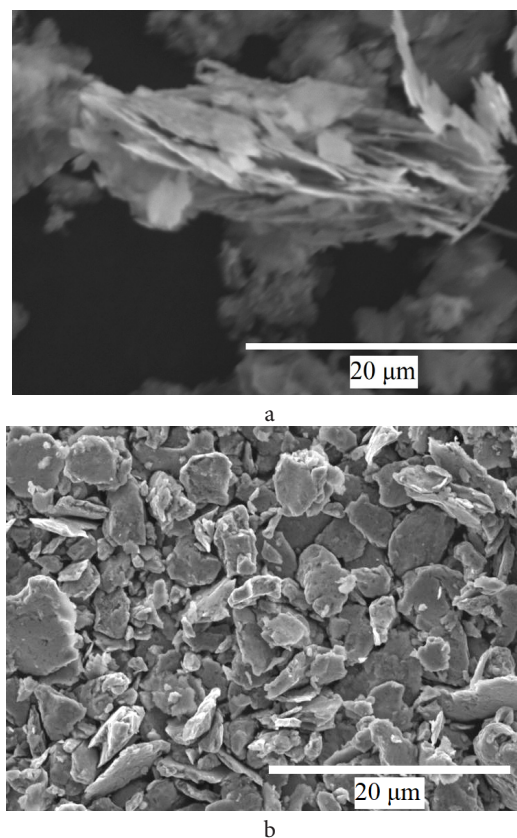

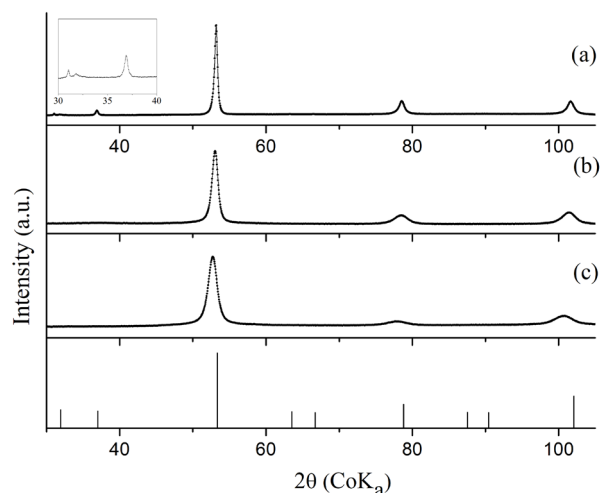**Fig. 1.** Electron microscopic images of samples 1 (a) and 2 (b).

Fig. 2. X-ray patterns of samples 1* (a), 1 (b), 2 (c).

Table 1. Lattice parameters of samples a and Si concentration in alloys C_{Si} in accordance with concentration dependences of lattice parameters of Fe-Si alloys [17, 18].

sample	a, nm, ± 0.0002	C_{Si}, at.%, ± 0.5
1*	0.2828	25
1	0.2837	22
2	0.2850	15

Table 2. Composition of surface layer of samples 1 and 2 (at.%).

sample	C	O	Fe	Si	Fe/Si
1	64	20	10	5	2
2	69	25	1	5	0.2

(Table 2). The Fe/Si ratio for the surface layers of sample 1 is 1.5 times smaller than it should be in accordance with the stoichiometric composition, while the silicon content in the surface layers of sample 2 is 15 times higher than it should be in accordance with the stoichiometric composition. This is associated with the fact that silicon atoms, which have a great affinity for oxygen, diffuse to the surface of the particles and form an oxide film enriched in silicon. This reason accounts for the decrease in the Si concentration in the volume of particles.

Presented in Fig. 3 are the Mössbauer spectra and hyperfine magnetic field distribution functions $P(H)$ of the samples. Partial disordering of the initial alloy can be caused by deformation in the attrition process during the preparation of the sample for the study (Fig. 3a). The Mössbauer spectra of 1 and 2 samples are typical of disordered crystalline solid solutions with non-magnetic sp-elements (Fig. 3b, c) [19]. A wide distribution of energetically nonequivalent local states of Fe atoms is observed.

Thus, the addition of the surfactant to the milling medium promotes the formation of plate-like particles with a thickness of about 0.5 μm. In the process of milling the alloy is disordered, the Si concentration in the alloy decreases to 22 at. %.

The particles produced by WBM in an acetone medium are plate-like particles with a thickness of not more than 2 μm and sizes of 1 – 10 μm. The silicon concentration in the alloy (15 at. %) is lower than the initial concentration, 25 at. %.
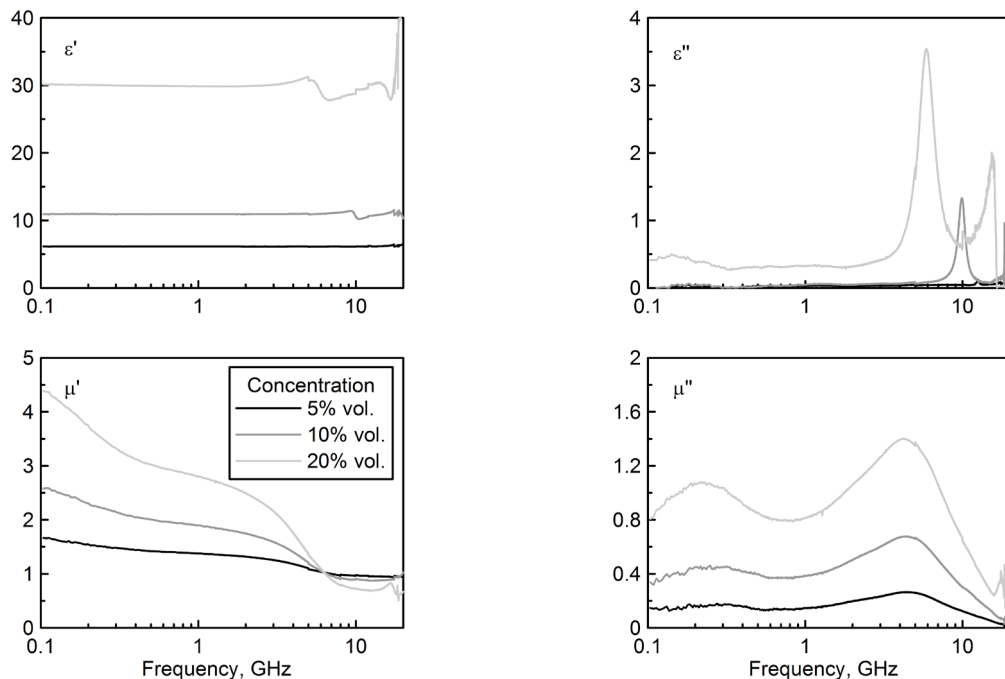
3.2. Microwave properties

The measured frequency dependences of the effective permeability and permittivity of composite samples filled with various volume fractions of the sample 1 powders are shown in Fig. 4. The frequency dependence of imaginary permeability has two distinct loss peaks. Fig. 5 shows the measured frequency dependences of the permittivity and permeability of the composites filled with various volume fractions of particles of sample 2.

The permittivity of the composites filled with sample 1 particles increases faster with increasing volume concentration than the permittivity of the composites with sample 2 particles. For both concentration series of the composites, a distinctive resonance-like behavior of the permittivity in a frequency range of 5 to 7 GHz is observed, which may be attributed either to the emergence and propagation of the higher-order modes in the coaxial sample [20] or to the resonance arising when the sample length is equal to the half of the wavelength in the sample material. Such resonance-like
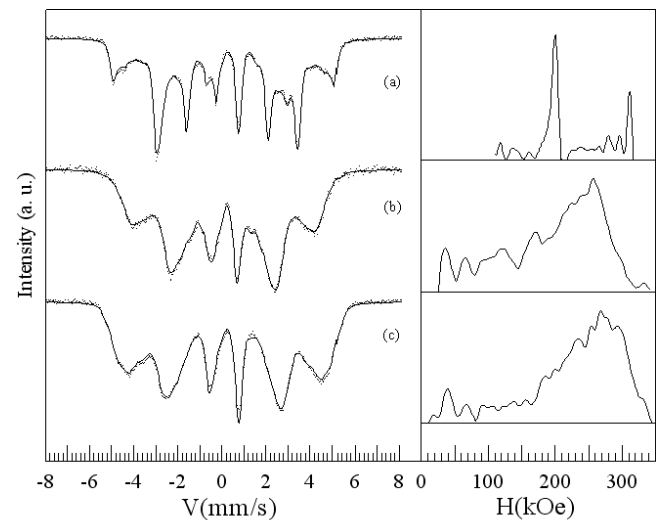
Fig. 3. Mössbauer spectra and hyperfine magnetic field distribution functions $P(H)$ of samples 1* (a), 1 (b), 2 (c).
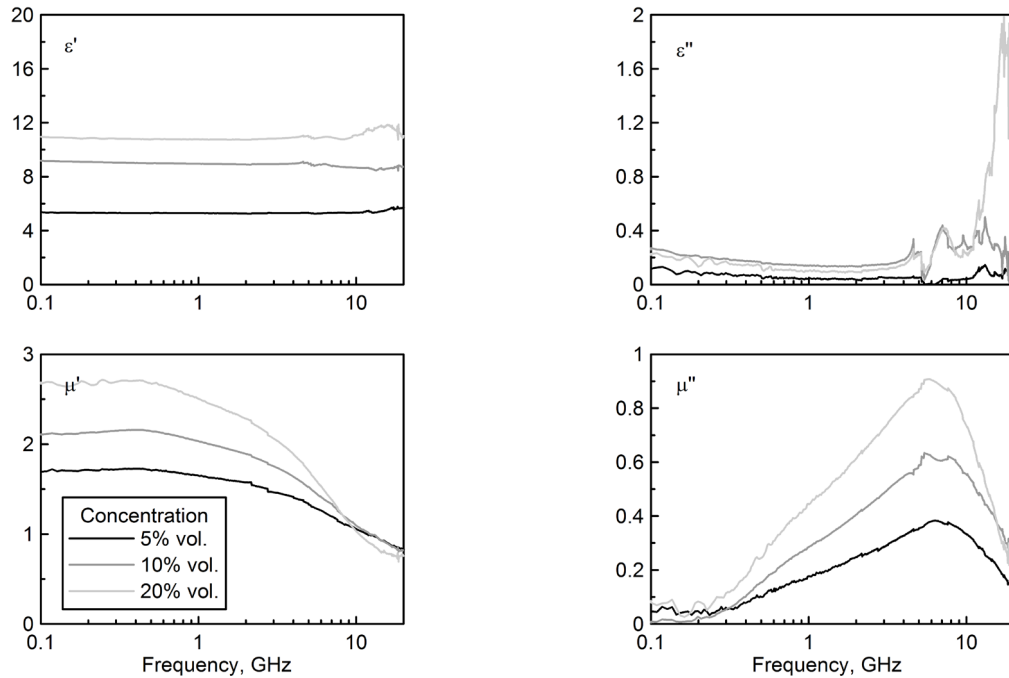

Fig. 4. The measured microwave permittivity (ε', ε") and permeability (μ', μ") of the composite samples filled with sample 1 powders with concentrations of 5% vol. (black), 10% vol. (gray) and 20% vol. (light-gray).

behavior is not critical for the further analysis, because, as it is well known, the permittivity of powder-filled composites is basically frequency-independent at microwaves (provided that the fraction of inclusions is not very high); for the permeability of the composites the resonance effects are less prominent.

The measured frequency dependences for composites with various volume concentrations were used to calculate the frequency dependence of the intrinsic permeability of the powder particles with the use of the Odelevsky mixing rule [21]. The result of the calculation is shown in Fig. 6. The depolarization factor, the static permeability and the percolation threshold were determined by fitting the measured low-frequency permittivity and permeability to the Odelevsky equation. Particles of sample 1 have a higher value of intrinsic permeability, lower values of depolarization factor and percolation threshold as compared to powder sample 2, see Table 3. With the use of the Lorentz function [22] for the approximation of the frequency dependences of the intrinsic permeability of the sample particles, the ferromagnetic resonance frequencies and Acher constants [23] were found. The axes ratio k of the depolarization ellipsoid [24] representing the effective particle in composites is also shown in Table 3.

Fig. 5. The measured frequency dependences of the complex permittivity and permeability of the composite materials filled with sample 2 powders with concentrations of 10% vol. (black), 15% vol. (gray) and 20% vol. (light-gray).
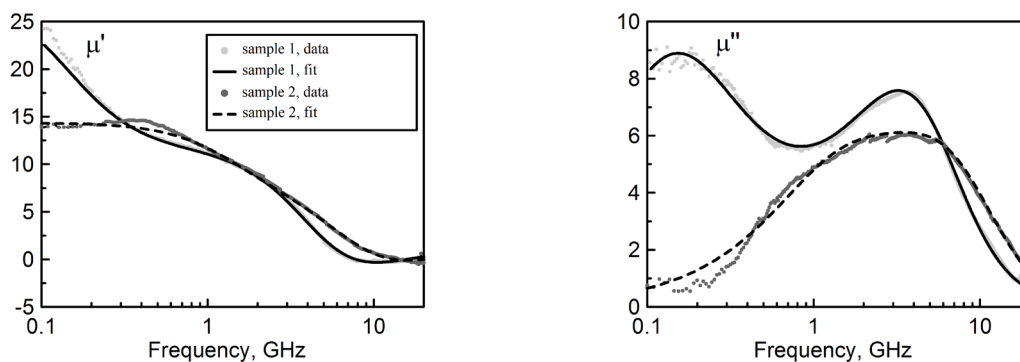
Fig. 6. The calculated frequency dependence of the intrinsic complex permeability of the particles of sample 1 (light-gray symbols — data, solid line — a fit of the calculated data by the Lorenzian frequency dependence) and sample 2 (dark gray symbols — data, dashed line — the fit).

Table 3. Parameters of powder particles derived from the concentration series of microwave permittivity and permeability of the composites with the use of the Odelevsky mixing rule.

powders	static permeability	depolarization factor	percolation threshold, vol. %	ferromagnetic resonance frequency, GHz	Acher constant, GHz^2	k ratio
sample 1	32	0.036	37	5.82	1045	21
sample 2	14	0.076	58	10.01	775	9

Both samples of particles have a plate-like shape, although the effective depolarization factor of sample 2 particles is half of that for particles of sample 1. This may indicate that particles in composites agglomerate differently, because the microwave measurements show a larger difference in the effective particle axes ratio k in composites (Table 3).

A substantial difference is seen in the microwave frequency dependences of the intrinsic permeability of powders and the effective permeability of composites with same volume concentration of powders. The imaginary permeability of particles of sample 1 have a pronounced peak in a frequency range of 0.1 to 0.2 GHz. The particles of sample 2 have two close peaks in the frequency range of 1 to 10 GHz and a reduced loss in the low-frequency region. The presence of low-frequency resonance is typical for composites filled with flake-like particles with a small effective depolarization factor [25, 13]. Possible reasons for this type of behavior may be the domain wall motion or the domain splitting of ferromagnetic resonance [25].

Conclusions

Fe-Si particles of a similar phase composition, but of various sizes and morphology can be produced by varying the composition of the milling medium (surfactant solution, acetone). The presence of a surfactant in the milling medium promotes the formation of plate-like particles about 0.5 µm in thickness. The use of acetone as a milling medium leads to the formation of plate-like particles of a larger thickness (approximately 2 µm).

The wet ball milling conditions are essential for the microwave magnetic properties of Fe-Si particles. Particles produced by surfactant-assisted milling have two distinct magnetic loss peaks and particles produced by wet ball milling in acetone have the peaks merged. Particles produced by surfactant-assisted milling have a higher static permeability and a lower resonance frequency.

The effective parameters of particles in composites determined with the use of the mixing rule indicate a difference in the agglomeration of particles. Composites made with particles produced with surfactant-assisted milling have agglomerates with a smaller depolarization factor. The low frequency peak of magnetic losses, which may be explained as a result of the domain walls motion, is strongly pronounced in composites with sample 1.

References

1. J. Ding, Y. Li, L. F. Chen, C. R. Deng, Y. Shi, Y. S. Chow, T. B. Gang. J. Alloy Comp. 314, 262 (2001). DOI: 10.1016/S0925-8388(00)01234-2
2. M. P. C. Kalita, A. Perumal, A. Srinivasan. J. Magn. Magn. Mater. 320, 2780 (2008). DOI: 10.1016/j.jmmm.2008.06.014
3. P. C. Shyni, P. Alagarsamy. Physica B. 448, 60 (2014). DOI: 10.1016/j.physb.2014.02.032
4. P. C. Shyni, A. Perumal. IEEE Trans. Magn. 50, 2101904 (2014). DOI: 10.1007/s003390050014
5. C. D. Stanciu, T. F. Marinca, I. Chicinas, O. Isnard. J. Magn. Magn. Mater. 441, 455 (2017). DOI: 10.1016/j.jmmm.2017.06.010
6. K. N. Rozanov, D. A. Petrov, E. P. Yelsukov, A. V. Protasov, A. S. Yurovskikh et al. Phys. Met. Metall. 117, 540 (2016). DOI: 10.1134/S0031918X16040116
7. Z. Zhang, J. Wei, W. Yang, L. Qiao, T. Wang, F. Li. Physica B: Condensed Matter. 406, 3896 (2011). DOI: 10.1016/j.physb.2011.07.019
8. M. Han, D. Liang, K. N. Rozanov, L. Deng. IEEE Trans. Magn. 49, 982 (2013). DOI: 10.1109/TMAG.2012.2227690
9. K. N. Rozanov, A. V. Osipov, D. A. Petrov, S. N. Starostenko, E. P. Yelsukov. J. Magn. Magn. Mater. 321, 738 (2009). DOI: 10.1016/j.jmmm.2008.11.039
10. C. Zhang, J. Jiang, S. Bie, L. Zhang, L. Miao, X. Xu. J. Alloy Comp. 527, 71 (2012). DOI: 10.1016/j.jallcom.2012.03.009
11. A. A. Shakov, D. A. Petrov, K. N. Rozanov, A. V. Syugaev, S. F. Lomaeva. Prot. Met. Phys. Chem. Surf. 53, 94 (2017). DOI: 10.1134/S2070205117010166
12. L. Cao, J.-T. Jiang, Z.-Q. Wang, Y.-X. Gong, Ch. Liu, L. Zhen. J. Magn. Magn. Mater. 368, 295 (2014). DOI: 10.1016/j.jmmm.2014.05.032
13. S. F. Lomayeva, A. V. Syugaev, A. N. Maratkanova, A. A. Shakov, K. N. Rozanov, D. A. Petrov, C. A. Stergiou. J. Alloys Comp. 721, 18 (2017). DOI: 10.1016/j.jallcom.2017.05.311
14. Powder Diffraction File. Alphabetical Index. Inorganic Phases. International Center for Diffraction Data, Swarthmore, PA, USA (1985).
15. O. M. Nemtsova. Nuclear Instruments and Methods in Physics Research Section B. 244(2), 501 (2006), DOI: 10.1016/j.nimb.2005.10.018
16. A. M. Nicolson, G. F. Ross. IEEE Trans. Instrum. Meas. 19, 377 (1970). DOI: 10.1109/TIM.1970.4313932
17. E. P. Yelsukov, V. A. Barinov, G. N. Konygin. Phys. Met. Metall. 62, 85 (1986).
18. V. M. Fomin, E. V. Voronina, E. P. Yelsukov, A. N. Deev. Mater. Sci. Forum. 269–272, 437 (1998). DOI: 10.4028/www.scientific.net/MSF.269-272.437
19. E. P. Elsukov, G. A. Dorofeev, A. I. Ul'yanov, A. V. Zagainov, A. N. Maratkanova. Phys. Met. Metall. 91, 258 (2001).
20. D. A. Petrov, K. N. Rozanov, M. Y. Koledintseva. Influence of Higher-order Modes in Coaxial Waveguide on Measurements of Material Parameters: Proc. 2018 Int. Symp. EMC+SIPI, Long Beach, CA, USA (2018).
21. S. N. Starostenko, K. N. Rozanov, A. O. Shiryaev, A. N. Shalygin, A. N. Lagarkov. J. Appl. Phys. 121, 245107 (2017). DOI: 10.1063/1.4989848
22. K. Rozanov, M. Koledintseva. Analytical representation for frequency dependences of microwave permeability: IEEE Symp. Electromagn. Compat. Pittsburg, PA (2012).
23. O. Acher, A. L. Adenot. Phys. Rev. B. 62, 11324 (2000). DOI: 10.1103/PhysRevB.62.11324
24. L. D. Landau, E. M. Lifshitz. Electrodynamics of Continuous Media, Course of Theoretical Physics. Pergamon Press Ltd. (1960).
25. T. Tsutaoka J. Appl. Phys. 93, 2789 (2003). DOI: 10.1063/1.1542651